Springer

Journal of
Mechanical
Science and
Technology

Journal of Mechanical Science and Technology 23 (2009) 1727~1735

www.springerlink.com/content/1738-494x
DOI 10.1007/s12206-009-0411-7

Aerodynamic analysis of flapping foils using volume grid deformation code †

Jin Hwan Ko[1], Jee Woong Kim[2], Soo Hyung Park[2,*] and Doyoung Byun[2]

[1]*School of Mechanical and Aerospace Engineering, Seoul National University, Seoul, South Korea*
[2]*Department of Aerospace Information Engineering, Konkuk University, Seoul, South Korea*

(Manuscript Received December 23, 2008; Revised March 7, 2009; Accepted March 17, 2009)

Abstract

Nature-inspired flapping foils have attracted interest for their high thrust efficiency, but the large motions of their boundaries need to be considered. It is challenging to develop robust, efficient grid deformation algorithms appropriate for the large motions in three dimensions. In this paper, a volume grid deformation code is developed based on finite macro-element and transfinite interpolation, which successfully interfaces to a structured multi-block Navier-Stokes code. A suitable condition that generates the macro-elements with efficiency and improves the robustness of grid regularity is presented as well. As demonstrated by an airfoil with various motions related to flapping, the numerical results of aerodynamic forces by the developed method are shown to be in good agreement with those of an experimental data or a previous numerical solution.

Keywords: Volume grid deformation; Computational fluid dynamics; Flapping foils; Finite macro-element; Transfinite interpolation

1. Introduction

As a nature-inspired technology, flapping foils have attracted much attention because they are capable to produce thrust with high efficiency. Flapping foils have been used as the thrust engine of micro-air vehicles. In design stage of the micro-air vehicles, computational fluid dynamics (CFD) is typically used for the numerical simulation of the flapping foils, but large motions of their surface boundaries should be considered. Therefore, it becomes a challenging problem in the CFD analysis to develop robust and efficient grid deformation algorithms appropriate for the large motion.

The grid deformation algorithms can be classified into linear algebra methods, elasticity-based approaches, and their hybrid forms. The linear algebra methods first generate the control points that are extracted from fluid grids by an exponential function and then translate the deformations of the control points to whole fluid grids by transfinite interpolation (TFI) [1], [2]. A Laplacian interpolation [3] and a local mesh adaptation [4] are also used to deform meshes in the same category. A spring analogy that uses tension and torsion springs based on the equation of continuum mechanics has been frequently used as an elasticity-based approach [5-7]. The spring analogy, however, is known to cause grid irregularity, and subsequently techniques for improving robustness of the grid regularity need to be developed. Recently, finite element method [8] and boundary element method [9] that uses the equilibrium equation of continuum mechanics have also been introduced for the grid deformation and are known to improve the grid irregularity. Between the two, the finite element based approach is known to be more suitable for interfacing to a computational fluid dynamics code that is implemented by finite volume method.

† This paper was recommended for publication in revised form by Associate Editor Do Hyung Lee

*Corresponding author. Tel.: +82 2 450 4177, Fax.: +82 2 444 6096
E-mail address: pish@konkuk.ac.kr

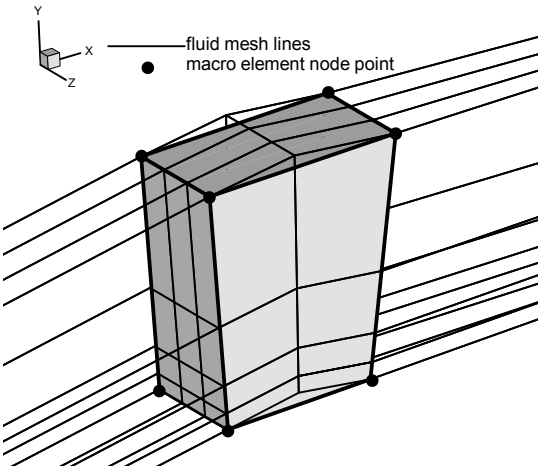

Fig. 1.Constitution of a macro-element.

In this study, a grid deformation code is developed based on the recently introduced approach that adopts a hybrid scheme of a finite element based method and a transfinite interpolation [10]. For the CFD analysis of the flapping foils, the grid deformation code then interfaces with a Navier-Stokes solver that finite volume method is implemented. The flapping foil is typically modeled by heaving and pitching harmonic motions with a phase angle [11]. For the validation of the presented code in use for the flapping foils, pitching [12], heaving [13], and both motion [13] are used for comparing with an experimental data or a previous numerical solution. First, the grid regularity is investigated when a pitching angle is varied with various conditions for generating the macro-elements imposed. Comparisons follow with experimental data or a previous numerical solution for the various motions in terms of aerodynamics force coefficients.

2. Volume grid deformation

The grid deformation we have developed is divided into two main procedures. First is to compute deformation from a finite macro-element model, and second is the transfinite interpolation that translates from the deformation of the macro-elements to whole fluid grids.

2.1 Generation and deformation of macro-finite element

Finite element based grid (or mesh) deformation approaches typically use entire fluid grids in constituting the finite macro-elements as depicted in Fig. 1. How to include the grid points in a macro-element is important for the preservation of the grid regularity. Here, we use the condition that satisfies minimum distance and minimum gird index number of each edge line of the macro-element. Details will be presented in results and discussion section.

The node displacements of the macro-elements are solved from an FE system equation with the constitutive relationship based on Hook's law.

$$\sigma_m = C_m \varepsilon_m \,, \tag{1}$$

where σ_m, ε_m are stress and strain vector, and

$$C_m = \begin{bmatrix} E_m & 0 & 0 & 0 & 0 & 0 \\ 0 & E_m & 0 & 0 & 0 & 0 \\ 0 & 0 & E_m & 0 & 0 & 0 \\ 0 & 0 & 0 & G_m & 0 & 0 \\ 0 & 0 & 0 & 0 & G_m & 0 \\ 0 & 0 & 0 & 0 & 0 & G_m \end{bmatrix}.$$

The effect of lateral deformation by Poisson's ratio is known to little contribute to the grid regularity; thus zeros are given in the off-diagonal terms of C_m. Young's modulus is given with the product of an artificial isotropic inhomogeneous constant E_0 and a weighting factor f_m. The spring analogy research shows that the grid regularity improves when the spring stiffness becomes large as the sampling points are closer to the moving boundary [6]. Thus the factor is given by an exponential form affected by the distance from the moving boundary:

$$E_m = E_0 f_m \quad , \quad G_m = \frac{1}{2} E_0 f_m \,, \tag{2}$$

where

$$f_m = \frac{1}{1 - \exp(-\beta \Delta r_m / r_{\max})}$$

in which Δr_m is the distance of the center of the macro element from the moving boundary and $r_{\max}$ is the maximum value of all Δr_m. The parameter β plays a role in controlling the change rate of the stiffness and is typically chosen between 1 and 6 [10]. The finite element system from Eq. (1) becomes the

linear algebra system with the prescribed boundary conditions:

$$\begin{bmatrix} K_{oo} & K_{os} \\ K_{so} & K_{ss} \end{bmatrix} \begin{bmatrix} U_o \\ U_s \end{bmatrix} = \begin{bmatrix} 0 \\ 0 \end{bmatrix}, \tag{3}$$

where U_o is unknown deformation vector and U_s is prescribed boundary condition vector corresponding to the moving boundary. Subscript *o* of *K* stands for quantity related to U_o and subscript s represents quantity related to U_s. Eq. (3) is then reduced to the linear system with only unknown vector:

$$K_{oo}U_o = -K_{os}U_s . \tag{4}$$

The deformation vector of this equation is solved by conjugated gradient iterative method with an incomplete factorization preconditioner.

2.2 Grid deformation by transfinite interpolation

Once the node displacements of the macro-elements are obtained, a transfinite interpolation is performed by using a blending function. The results are known to be a continuity of displacements at all macro-element boundaries, even if continuity of the derivative of the displacement is not ensured [10]. A blending function in public domain, BLEND[14], is employed. BLEND is coded by C and FORTRAN languages and is released in the function that interpolates corresponding fluid grids from a macro-element by using the deformations of the edge points. The moving boundary, however, is composed of surfaces in three-dimension; thus we need to modify the original code for translating the fluid grids from given displacements over the surface of the macro element. Except for the modification, we straightforwardly adopt the subroutines of BLEND.

Through the two separate procedures, large motions over a moving boundary successfully are imposed upon the whole fluid grids. The grid deformation is developed for three-dimensional structured grids and is referred to as volume grid deformation (VGD).

3. Computational fluid dynamics with VGD

3.1 Computational fluid dynamics code

As mentioned previously, numerical simulation for obtaining aerodynamic forces will be done by a computational fluid dynamics code. KFLOW, which we adopt, is an in-house code for the three-dimensional compressible, preconditioned Navier-Stokes analysis. Multi-block structured grid and automated interpolation point generation algorithm are implemented and can be applied to Chimera grid[15]. Spatial discretization is done by finite volume method where discretization schemes with second and fourth order accuracy and WENO (Weighted Essentially Non-Oscillatory) scheme with fifth order accuracy are implemented. Spalart Allmaras, k-ω Wilcox, k-ω Wilcox Durbin (WD+), k-ω SST (Shear Stress Transport), and k-ε Launder-Sharma turbulence models are available[16].

3.2 Interface between KFLOW and VGD

The modules and data flow of VGD coupled with KFLOW are depicted in Fig. 2. For the CFD analysis of a flapping foil, the CFD solver should consider the large deformation of moving boundaries. As aforementioned, VGD plays a role in computing the deformation of the entire fluid grids from the displacement of the moving boundaries, which is made by a motion generator in Fig. 2. One cycle with KFLOW, motion generator, and VGD is performed at each time step. The surface grid of the moving boundaries to the motion generator is transferred only at starting time step, because the surface is not deformed for the current applications. Displacements of the moving boundaries and deformations of the fluid grids are updated at each time step and eventually aerodynamic forces are acquired by KFLOW. Each cell volume of the fluid grid is changed as a function of time, whereas the volume from the rigid rotation approach is not changed. The current dynamically deforming grid approach may cause an accumulation of the numerical error or violate the geometric conservation law (GCL) on varying cell volumes. See reference[17] for more details. To eliminate the error the geometric conservation law is enforced at each time step:

$$\frac{\partial V_i}{\partial t} \cong \frac{3V^{n+1} - 4V^n + V^{n-1}}{2\Delta t} = \oint_{\partial S} \vec{V}_g \cdot d\vec{S} , \tag{5}$$

where V is the cell volume, Δt is the time step, and $\vec{V}_g$ denotes the grid velocity of the moving mesh.

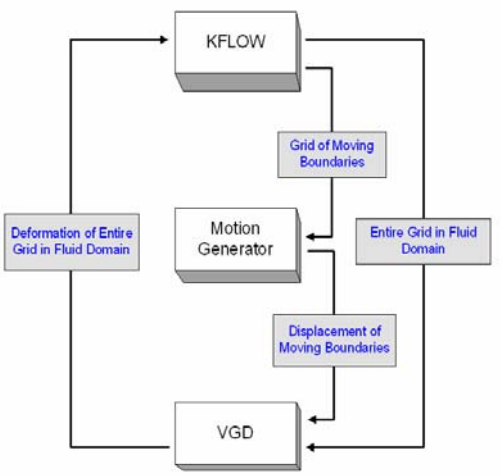

Fig. 2. Modules and data flow when VGD interfaces with KFLOW.

3.3 Kinematics of a flapping foil

The real flapping motion of an insect or a bird is represented by a complex kinematics. To analyze aerodynamic forces experimentally or numerically, the flapping motion is typically modeled by heaving and pitching motions. $y(t)$ is denoted by the vertical position of the heave position with zero corresponding to the mid-depth as shown in Fig. 3, which is brought from the flapping kinematics of Ref. [11]. The pitching angle $\theta(t)$ is the angle between the direction of velocity V and foil chord. In this study, harmonic foil motions are simply adopted as

$$\begin{aligned} y(t) &= y_0 \sin(\omega t) \\ \theta(t) &= \theta_i + \theta_0 \sin(\omega t + \delta) \end{aligned} \quad (6\text{-}1)$$

or

$$\begin{aligned} y(t) &= y_0 \cos(\omega t) \\ \theta(t) &= \theta_i + \theta_0 \cos(\omega t + \delta) \end{aligned}, \quad (6\text{-}2)$$

where y_0 and θ_0 are the maximum heave position and the maximum pitching angle, and δ is the phase angle between heave and pitch. θ_i is the initial angle and ω is the frequency in radian, which is equal to $\omega = 2\pi f$, where f is the flapping frequency.

4. Numerical experiments

4.1 Constitution of macro-element and its regularity

We first investigate the preservation of the grid regularity under a pitching motion when a condition for

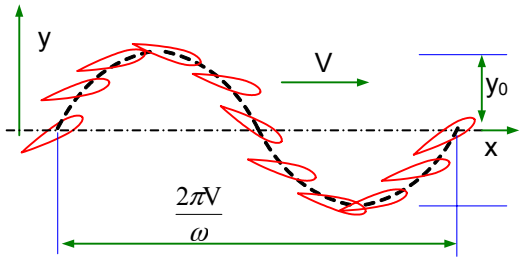

Fig. 3. Kin ematical motion of a flapping foil.

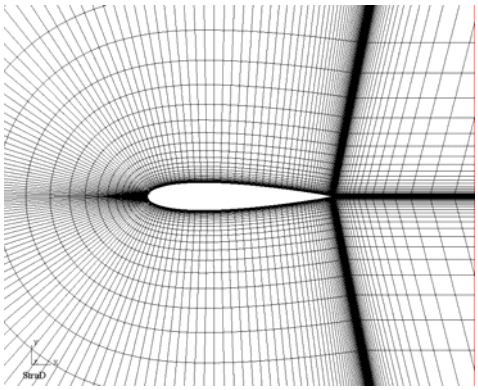

Fig. 4.Original grid of NACA0015 airfoil.

generating macro-elements is varied. The grid system of NACA0015 airfoil in Fig. 4 is used. The number of meshes is 290,080 and the minimum length of grid edge is 10^{-4}. β is known to have minor effect on the gird regularity and then is fixed to 6.

First, the minimum number of grid index (MNG) condition of macro-element is imposed, but the minimum distance condition is not imposed.

The results of the gird regularity are listed in Table 1 when MNG is varied by 3, 6 and 9 with the pitching angle changed from 10 to 60 with the increment 10. In Table 1, the second column contains the number of generated macro-elements, 'o' means that the grid regularity is preserved and 'x' means that the grid regularity is not.

It is indicated from Table 1 that the numbers of the macro-elements are much smaller than the number of the fluid grids, but the grid regularities for all MNG numbers are broken at the pitching angle of 30 degrees. For instance, 6 MNG, which generate 1,944 macro-elements, is depicted in Fig. 5. A large aspect ratio of the macro-elements is observed and the discrepancies in mesh size are large, as shown in Fig. 5. The large aspect ratio and the discrepancies cause the mesh irregularity in Table 1.

Table 1. Preservation of the grid regularity with MNG condition.

MNG	Elm#	Pitch angle					
		10	20	30	40	50	60
3	12,138	x	x	x	x	x	x
6	1,944	o	x	x	x	x	x
9	648	o	o	x	x	x	x

Table 2. Preservation of the grid regularity with MDE condition.

MDE	Elm#	Pitch angle					
		10	20	30	40	50	60
0.03	53,592	o	o	o	o	o	x
0.06	15,600	o	o	o	o	o	x
0.09	7,488	o	o	o	o	o	o

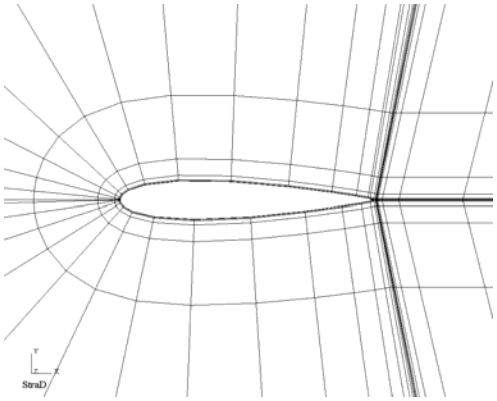

Fig. 5. Generated macro-elements with MNG condition.

Second, the minimum edge distance (MDE) condition of the macro-element is imposed but MNG condition is not imposed. The results of the grid regularity are listed in Table 2 when MDE is varied by 0.03, 0.06, and 0.09 with the pitching angle changed from 10 to 60 degrees with an increment of 10.

It is shown in Table 2 that the robustness of grid regularities improves, but the number of the macro-elements much increases as compared to the first case. The large number of the macro-elements has an unfavorable effect on the efficiency of VGD.

Fig. 6, in which 15,600 macro-elements are generated with MDE 0.06, shows that unnecessarily many macro-elements are generated far away from the moving boundary of the grid system.

Finally, we impose both MNG and MDE conditions. The results of the gird regularity are listed in Table 3

Table 3. Preservation of the grid regularity with MDE and MNG condition.

MNG,MDE	Elm#	Pitch angle					
		10	20	30	40	50	60
3, 0.03	4,312	o	o	o	o	o	o
6, 0.06	720	o	o	o	o	o	o
9, 0.09	264	o	o	o	o	o	o

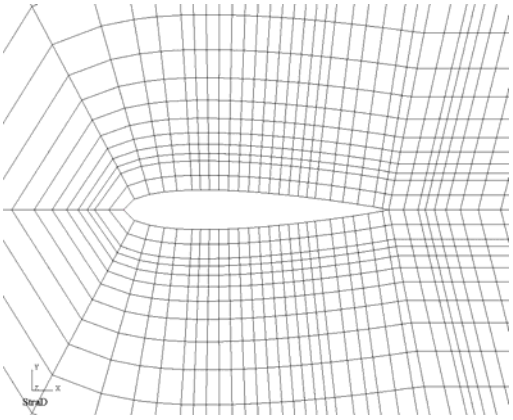

Fig. 6. Generated macro-elements with MDE condition.

when (MNG, MDE) are varied by (3, 0.03), (6, 0.06), and (9, 0.09) with the pitching angle changed by from 10 to 60 degrees with an increment of 10.

It is indicated from Table 3 that the grid regularities improve and also the number of the macro-elements is small, which inherits the advantages of both previous conditions. Too small a number of the macro-element can cause a large interpolation error; thus (3, 0.03) case is selected in the next validation problems. Fig. 7, in which 4,312 macro-elements are generated with (MNG, MDE) equal to (3, 0.03), shows that both conditions generates macro elements with the smaller aspect ratio and prevent the generation of the unnecessarily many macro-elements far away from the moving boundary.

Fig. 8 shows the deformed macro-elements and fluid grids near the trailing edges, at which the grid deformation is most serious, when the airfoil is instantaneously pitched to 60 degrees. In Fig. 8 the orientations of the fluid grids, namely, the grid regularities, are preserved even at a pitch of 60 degrees.

4.2 Validation for a pitching motion

Navier-Stokes calculation was performed for a pitching NACA0015 in order to validate the developed VGD code, and its results were then compared

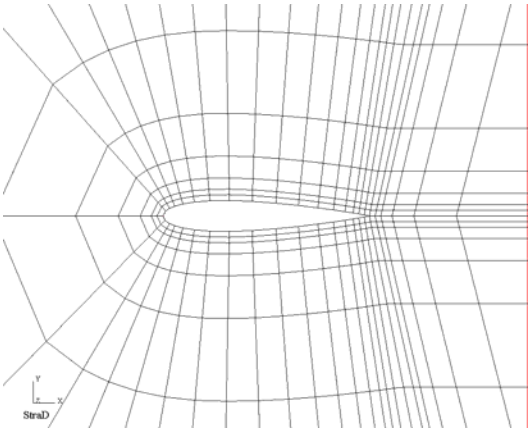

Fig. 7. Macro-elements with both conditions.

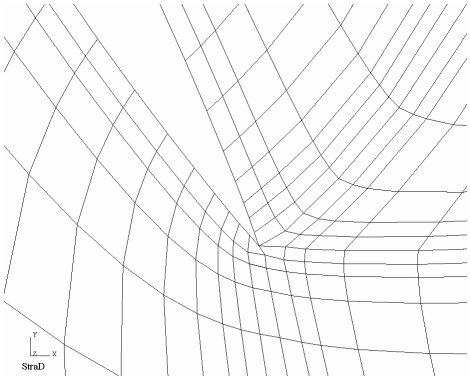

(a) Macro-elements

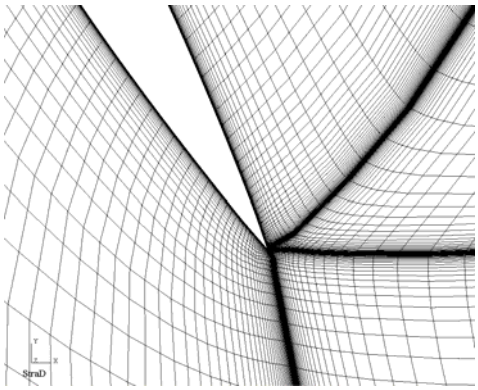

(b) Fluid grids

Fig. 8. Deformed macro-elements and fluid grids near the trailing edge at 60 degree pitch.

with the experimental results of Piziali [12], in which the maximum and minimum angles are 8.2 and -0.2 are used: $\theta_i = 4$, $\theta_0 = 4.2$ of Eq. (6-2).

In detail, the grid deformation was generated from

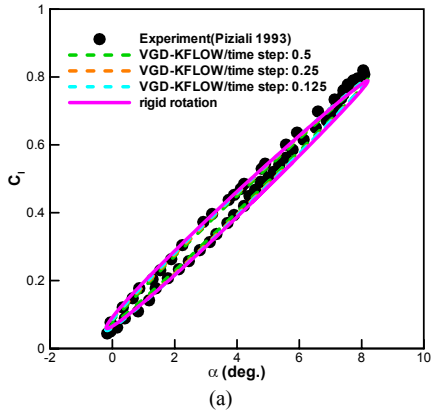

(a)

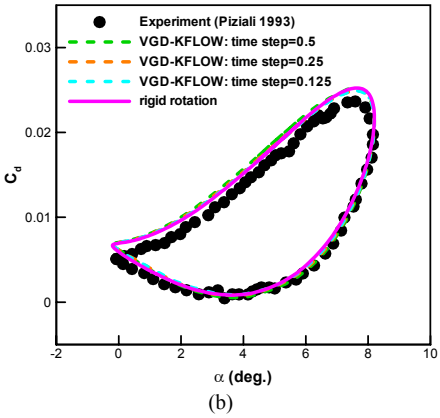

(b)

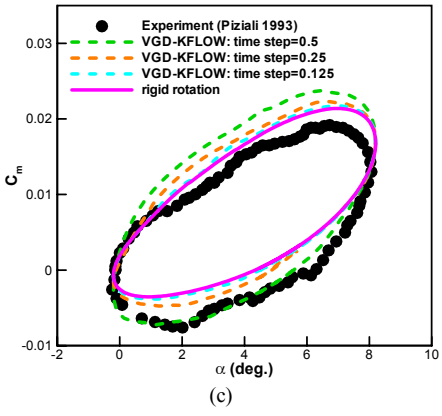

(c)

Fig. 9. Hysteresis loops of (a) lift, (b) drag, and (c) moment coefficients when the airfoil is pitched from -0.2 to 8.2 degrees.

VGD by imposing the pitching motion only on the airfoil surface and fixing the far field boundary, and was also compared with those of rigid rotation. Mach number is 0.29, Reynolds number is 1.95×10^6, and reduced frequency ($= 2\pi fc/U_\infty$) is 0.2. Non-dimensional time ($= tc/U_\infty$) is 32 in a period and the

non-dimensional time step is varied by 0.5, 0.25, and 0.125. The unsteady computations were performed during three cycles at least, and the converged and periodic behavior is observed from the third period. K-ω Wilcox Durbin (WD+) turbulence model is applied to the unsteady turbulent computation[16]. The comparison among results of the experiment, rigid rotation and the developed code with the chosen parameters in the previous section is shown in Fig. 9.

As shown in Fig. 9, the results from the VGD and the rigid rotation with time step of 0.125 well agree with the experimental results. It is also shown that the computational results become close to the experimental results as the time step gets smaller.

In particular, the moment by the VGD is considerably affected by the variation of the time step, but the VGD results at time step, 0.125, are almost equal to results of the rigid rotation; thus, it is difficult to assume that the discrepancies of the VGD results with the smaller time steps are due to geometric conservation law. The discrepancies are too large to obtain a time-step convergence, unless the geometric conservation law is enforced. It is observed that the main discrepancies occur at pitch-up; thus, it is speculated that with the dynamically deforming grid the vortices developed at pitch-down cause these discrepancies by interacting with the airfoil surface. Hence, researches on the sensitivity of grids and numerical variables will be required to explore the reason for these discrepancies.

4.3 Validation for a heaving motion

NACA0012 airfoil is employed to compare the lift and thrust coefficients with a previous numerical solution [13]. In the following computations, a C-type grid with $384 \times 61 \times 5$ points, in which far-field boundaries are located far from 10 chord length, is used. The amplitude of a heaving motion in Eq. (6-2) is $y_0 = -0.175c$, the reduced frequency is 4.58, Mach number is 0.05 and Reynolds number is 2.0×10^4. The time history of lift and thrust coefficients, which is equal to negative of the drag coefficient, are depicted in Fig. 10 where a Navier-Stokes solution (NS) [13] is used as reference solution.

As shown in Fig. 10, the Navier-Stokes solutions by VGD-KFLOW are in good agreement with the NS solutions. All aerodynamic forces exhibit a periodic behavior and the frequency of the variation of the thrust coefficient is two times larger than that of the lift coefficient, since the maximum thrust occurred as the airfoil passed the mean position twice in one period.

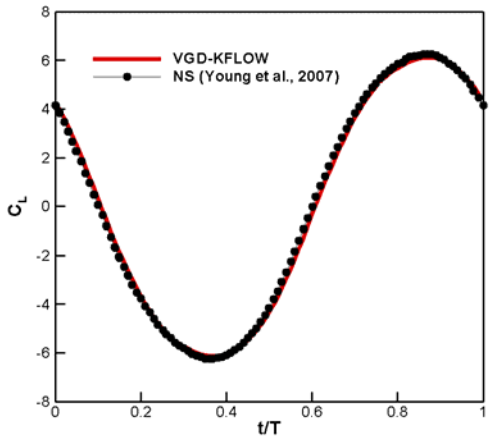

(a) Lift coefficient

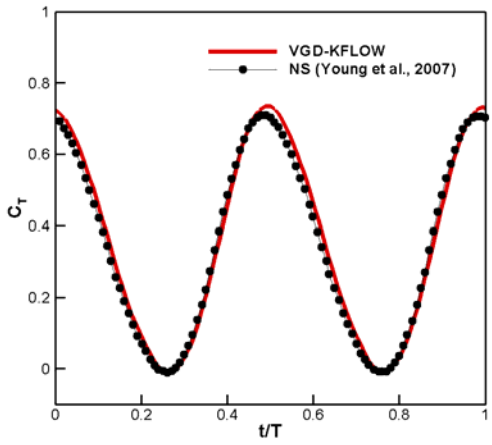

(b) Thrust coefficient

Fig. 10. Force coefficients of heaving motion with 0.175c amplitude.

4.4 Validation for a heaving and pitching motion

NACA0012 airfoil, for which the same grid system of the heaving motion is used, with both heaving and pitching motion is employed to compare time-varying thrust force and lift forces with a previous Navier-Stokes (NS) result[13]. The Navier-Stokes computation is performed by using fully laminar flow, where Mach number is 0.05 and Reynolds number is 40,000. Strouhal number is given by 0.1, which is low. The heaving and pitching motions are driven by Eq. (6-2), in which the pivot point is located at the 1/3 chord point, pitch amplitude is 2.48 degrees with zero initial

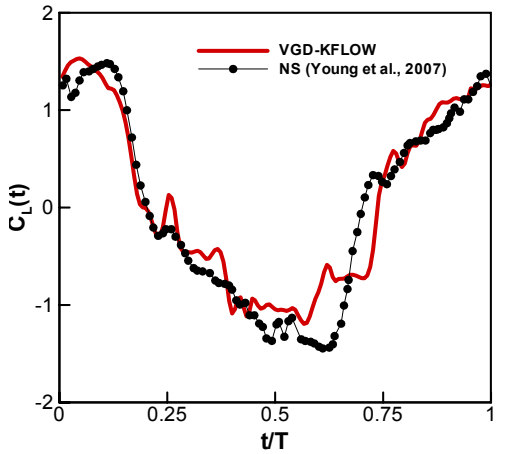

(a) Lift coefficient

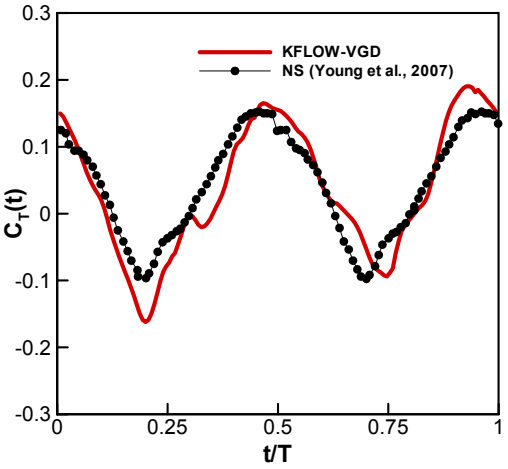

(b) Thrust coefficient

Fig. 11. Force coefficients of the heaving and pitching motions.

pitch, heave amplitude is 0.75c, and phase angle δ is 90 degrees. The VGD-KFLOW and the previous NS results are depicted in Fig. 11. As shown in Fig. 11, the VGD-KFLOW lift and thrust coefficients agree with the NS solution of Young et al., whereas irregular oscillations about the underlying sinusoidal behavior are seen. The irregularity is caused from the unsteady vortices that are separated from leading-edge boundary layer. The leading-edge vortices significantly alter the flow field on the airfoil, especially the pressure distribution. It is found that the VGD-KFLOW supplies unaltered grid spacing near the airfoil surface so that there is little geometrical change near the moving boundary. Young et al.[13] applied nearly the same grid density but smaller time step than that of the present computation. It is possible to apply larger time step to the unsteady computation, since VGD-KFLOW allows more flexible grid deformation. More precise computations and analysis are needed to validate the computational results. The present verification study shows that the present volume grid deformation code provides robust and efficient grid movement for numerical simulations of flapping foils with relatively large motions.

5. Conclusion

A volume grid deformation has been developed based on finite Macro-Element and transfinite interpolation and then successfully interfaced with a structured multi-block Navier-Stokes solver. As demonstrated by an airfoil with a pitching motion, the orientation of the fluid grid, which is a measure of the grid regularity, is preserved even at the pitching angle of 60 degrees. When an airfoil is excited by pitching, heaving, and the coupled motion, the aerodynamic force coefficients related to thrust of the developed code are in good agreement with those of experimental data and previous numerical solutions. The present volume grid deformation code is expected to be an efficient analysis tool due to the enhanced macro-element scheme, when predicting the aerodynamic forces of rigid or deformable flapping foils.

Acknowledgment

This work was supported by the faculty research fund of Konkuk University in 2007.

References

[1] P. M. Hartwich and S. Agrawal, Methods for Perturbing Multi-block Patched Grids in Aero-elastic and Design Optimization Applications, *AIAA paper* 97-2038 (1997).

[2] M. A. Potsdam, G. P. Guruswamy, A parallel multi-block movement scheme for complex aero-elastic applications, *39th AIAA Aerospace Science Meeting and Exhibit*, AIAA 2001-0716, January 8-11, Reno, NV (2001).

[3] S. Z. Su, L. Liu, H. Zhang, and D. Zhang, Numerical Simulation of Vortex-induced Vibration of a Square Cylinder, *Journal of Mechanical Science and Technology* 21 (2007) 1415-1424.

[4] D. J. Kang and S. S. Bae, Frequency effects of upstream wake and blade interaction on the unsteady

boundary layer flow, *KSME International Journal* 16 (10) (2002) 1303-1313.

[5] J. T. Batina, Unsteady Euler Airfoil Solutions Using Unstructured Dynamic Meshes, *AIAA Journal* 28 (8) (1990) 1381-1388.

[6] F. J. Blom, Considerations on the spring analogy, *International Journal for Numerical Methods in Fluids* 32 (2000) 647-668.

[7] K. Nakahashi and G. S. Deiwert, Three-Dimensional Adaptive Grid Method, *AIAA Journal* 24 (6) (1986) 948-954.

[8] E. J. Nielsen and W. Kyle Anderson, Recent Improvement in Aerodynamic Design Optimization on Unstructured Meshes, *39th AIAA Aerospace Sciences Meeting and Exhibit*, January, Reno NV, AIAA-2001-0596 (2001).

[9] X. W. Gao, P. C. Chen and L. Tang, Deforming Mesh for Computational Aeroelasticity Using a Nonlinear Elastic Boundary Element Method, *42th AIAA/ASME/ASCE/AHS/ASC Structures, Structural Dynamics, and Materials Conference and Exhibit*, Seattle, WA, AIAA 2001-25295 (2001).

[10] R. E. Bartels, Finite Macro-Element Mesh Deformation in a Structured Multi-block Navier-Stokes Code, *NASA Technical Memorandum* 2005-213789 (2005).

[11] L. Schouveiler, F. S. Hover and M. S. Triantafyllou, Performance of flapping foil propulsion, *Journal of Fluids and Structures* 20 (2005), 949-959.

[12] R. A. Piziali, An experimental investigation of 2D and 3D oscillating foil aerodynamics for a range of angle of attack including stall, *NASA Technical Memorandum* 4632 (1993).

[13] J. Young, J. C. and S. Lai, Mechanisms influencing the efficiency of oscillating airfoil propulsion, *AIAA Journal* 45 (7) (2007) 1695-1702.

[14] J. Thompson, B. Soni, and N. Weatherill, *Handbook of Grid Generation*, CRC Press (1999). The code of transfinite interpolation is released at http://people.scs.fsu.edu/~burkardt/cpp_src/blend/blend.html.

[15] S. H. Park, Prediction Methods of Dynamic Stability Derivatives Using the Navier-Stokes Equations, PhD thesis: Korea Advanced Institute of Science and Technology (2003).

[16] S. H. Park and J. H. Kwon, Implementation of k-ω Turbulence Models in an Implicit Multigrid Method, *AIAA Journal* 42 (7) (2004) 1348-1357.

[17] P. D. Thomas and C. K. Lombard, Geometric Conservation Law and Its Application to Flow Computations on Moving Grids, *AIAA Journal* 17 (1979) 1030-1037.

Jin Hwan Ko received his B.S. degree in Mechanical Engineering from KAIST, Korea, in 1995. He then received his M.S. and Ph.D. degrees from KAIST in 1997 and 2004, respectively. Dr. Ko is currently a research professor at the School of Mechanical and Aerospace Engineering at Seoul National University in Seoul, Korea. His research interests include fluid-structure interaction analysis, structural dynamics of a micro-scale resonator, and model order reduction.

Soo Hyung Park received his B.S. degree in Aerospace Engineering from KAIST, Korea, in 1996. He then received his M.S. and Ph.D. degrees from KAIST in 1999 and 2003, respectively. Prof. Park is currently an assistant professor at the Dept. of Aerospace Information Engineering at Konkuk University in Seoul, Korea. His research interests include computational fluid dynamics, fluid-structure interaction analysis, rotorcraft aerodynamics, and turbulence modeling.